CrossMark

ORIGINAL RESEARCH

Coconut oil-cellulose beaded microfibers by coaxial electrospinning: An eco-model system to study thermoregulation of confined phase change materials

W. M. Ranodhi N. Udangawa (iD) · **Charles F. Willard** · **Chiara Mancinelli** · **Caitlyn Chapman** · **Robert J. Linhardt** (iD) · **Trevor John Simmons** (iD)

Abstract Coconut oil was used to produce biomass microfibers with a coconut oil core and a cellulose shell by a co-axial electrospinning technique. This novel material was developed as a model system to determine the effect of confining a phase changing material within an axial micropore of a coaxial fiber. The morphology of these composite fibers was determined by scanning electron microscopy and transmission electron microscopy, which revealed a unique beaded necklace morphology with sub-micron scale pockets of confined coconut oil. Thermogravimetric analysis and differential scanning calorimetry were employed to study the thermal behavior of the composite fibers. A significant increase of the specific heat capacity ($+98\%$) was observed when the coconut oil was confined within the micropore of the composite fiber compared to the bulk. There was also a notable increase ($+41\%$) of the specific heat of melting for the micropore confined coconut oil. Thus, coconut oil isolated in the axial micropore core of these cellulose composite fibers showed excellent potential for temperature regulation in the range of 7 to 22 °C, which includes 21 °C, the temperature which most humans find comfortable. The results of the studied model system can be used to tailor the properties of phase change materials in confined micropores, in both electrospun fibers and other mesoscale structures.

W. M. R. N. Udangawa (✉) · C. Mancinelli · C. Chapman · R. J. Linhardt
Department of Chemistry and Chemical Biology, Rensselaer Polytechnic Institute, Troy, NY 12180-3590, USA
e-mail: simmot@rpi.edu

W. M. R. N. Udangawa · R. J. Linhardt
Center for Biotechnology and Interdisciplinary Studies, Rensselaer Polytechnic Institute, Troy, NY 12180-3590, USA

C. F. Willard · R. J. Linhardt
Department of Chemical and Biological Engineering, Rensselaer Polytechnic Institute, Troy, NY 12180-3590, USA

R. J. Linhardt
Rensselaer Nanotechnology Center, Rensselaer Polytechnic Institute, Troy, NY 12180-3590, USA

R. J. Linhardt · T. J. Simmons
Heparin Applied Research Center, Rensselaer Polytechnic Institute, Troy, NY 12180-3590, USA

Graphical abstract
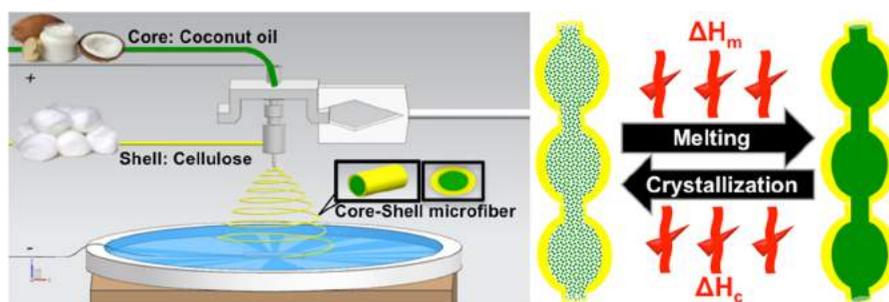
Introduction

Human beings are homeothermic, maintaining a core body temperature of 37 °C through metabolic and physiologic processes (Flouris and Cheung 2006). Changes in metabolic rate are generally an efficient thermoregulation mechanism in response to temperature changes in the external environment. According to the standards published by the American Society of Heating, Refrigerating and Air-conditioning Engineers (ASHRAE) in 2010, metabolic rate is defined as the level of transformation of chemical energy into heat and mechanical work by metabolic activities within an organism. Despite this response in metabolic rate, temperature changes in the immediate microclimate of an individual can cause extreme discomfort and stress, particularly in professions that require protective body armor and other bulky clothing, thus, resulting in a decline in work performance (Cadarette et al. 2006). Temperatures between 18 and 21 °C are considered to be the most comfortable temperatures for living rooms and public spaces, respectively (Boardman 2013; Walker 2009).

In cold climates, heating, used for centuries, has relied on a variety of fuel sources. In warmer climates, in the last century, air conditioning has been used to achieve this comfort level at a cost of electric and fossil fuel energy. The residential, commercial and industrial use of air conditioning is notably rising due to the increasing population and global warming. According to the US Department of Energy, roughly 117 million metric tons of carbon dioxide is released into the air each year as a result of increasing air conditioning usage. This could further accelerate the adverse effects on the environment, thus causing climate change. Hence, the concept of creating wearable materials that can regulate body temperature has drawn increased attention of researchers over the past few decades (Meng et al. 2015).

Phase changing materials (PCMs) have been used to produce smart textiles since the 1980's to regulate temperature of the wearer (Vigo and Frost 1982, 1983). PCMs have the capability to store and release latent heat energy as they undergo phase changes while keeping their temperature constant (Chen et al. 2007). PCMs can be divided into three main groups: organic, inorganic and eutectics depending on the chemical nature of the material (Abhat 1983; Hasnain 1998; Nejman and Goetzendorf-Grabowska 2013). Organic PCMs are non-corrosive (Mondal 2008), recyclable and show low vapor pressure of melting (Fang et al. 2010; Farid et al. 2004). Paraffin wax, mineral oil, fatty acids and polyethylene glycol are few examples of organic PCM (Nejman and Goetzendorf-Grabowska 2013). Inorganic PCMs are hydrated salts that have high thermal conductivity and a wide range of melting temperatures (Mondal 2008). Eutectic PCMs are mixtures of two or more organic and/or inorganic components that can melt and freeze without any segregation (Abhat 1983; Nejman and Goetzendorf-Grabowska 2013).

Initially, inorganic salt hydrates were mixed into textile fibers such as rayon to modify the heat capacities of the fibers to impart thermo-regulating properties (Vigo and Frost 1982). Use of salts were

subsequently replaced with polymeric materials to produce more durable composite fibers (Vigo and Frost 1983). Several types of polymeric nanocomposite fibers have been fabricated by electrospinning (Chen et al. 2007, 2011), in which one polymer is used as the matrix and the other functions as a PCM. Even though general mixing of PCMs with other polymers works for the most part (Chen et al. 2007), encapsulation of the PCMs inside polymers prevents leaching of the PCMs, thereby ensuring the durability of the material. Outlast Technologies, one major provider of phase change fabrics, recently introduced a thermo-regulating textile fiber-composite consisting of textile yarns injected with microencapsulated PCMs called Thermocules® (Coyle et al. 2007; Iqbal and Sun 2014; Nelson 2002).

Electrospinning is a fiber fabrication technique that was invented nearly a century ago (Cooley 1902). Conventional electrospinning involves dissolution of the desired polymer in a volatile solvent that evaporates in the electrospinning process leaving dry polymeric fibers on a solid collector, commonly known as wet-dry electrospinning (Chen et al. 2010; Hou et al. 2016; Lalia et al. 2013). Electrospinning complex polysaccharides, such as cellulose, is challenging due to the insolubility of cellulose in water or most volatile organic solvents (Meli et al. 2010). Cellulose, a linear polysaccharide with an extensive hydrogen-bonding network, possesses excellent thermal and mechanical properties allowing it to form fibers with high tensile strength (Hou et al. 2016; Khalil et al. 2012). While its strong intra and intermolecular hydrogen-bonding prevents the dissolution of cellulose in conventional solvents (Liebert 2010), a class of non-volatile, hydrogen-bond-breaking solvents known commonly as room temperature ionic liquids (RTILs) readily dissolve cellulose and can be used in electrospinning (Farrán et al. 2015; Meli et al. 2010; Simmons et al. 2011; Viswanathan et al. 2006). RTIL-dissolved cellulose can be electrospun into a coagulation bath filled with water, a non-solvent that is miscible with the RTIL but which does not dissolve cellulose. This process is referred to as wet–wet electrospinning (Freire et al. 2011; Meli et al. 2010; Miao et al. 2011; Teo and Ramakrishna 2006; Zheng et al. 2014).

Our goal is to develop a one-step process to inexpensively encapsulate biocompatible PCM inside a cellulose matrix that can be adapted to a wide variety of 'green' polymers. Electrospinning is selected because of its widespread use in fabricating polymeric composites in industry. We hypothesize that confining coconut oil in the core of a cellulose fiber could result in a robust phase change material and could produce a beneficial impact on the thermal properties of the coconut oil through confinement.

In the current study, hollow cellulose microfibers are used as a solid supporting sheath to hold coconut oil, which acts as the phase changing material. These novel electrospun composite fibers are created by the wet–wet/melt/co-axial electrospinning (McCann et al. 2006) method. Cellulose is the most abundant biopolymer on earth (Arioli et al. 1998; Swatloski et al. 2002) making this composite both inexpensive and biodegradable (Frenot et al. 2007). Co-axial electrospinning isolates coconut oil in the microfiber core surrounded by a cellulose shell (Huang et al. 2015; Lan et al. 2015; Yu et al. 2013a, b). Multi-axial electrospinning techniques require multi-nozzle spinnerets that allow fabrication of fibers with multiple materials in contrast to mono-axial electrospinning (Li et al. 2010).

Coconut oil is an inexpensive and sustainable natural alternative to other more expensive PCMs such as inorganic salts (Vigo and Frost 1982) and synthetic polymers (Vigo and Frost 1983). It is extracted from the kernel/meat of mature coconut harvested from the coconut palm tree, *Cocos nucifera,* and consists of a mixture of saturated fatty acids (51% is lauric acid) (Jayadas and Nair 2006). In contrast to most vegetable oils, coconut oil has a pour point as high as 24 °C (Ajithkumar et al. 2009). It is an edible oil with many health benefits and a wide range of applications in food, cosmetics, lubricants, and biodiesel industries (Jaganathan and Fauzi Ismail 2017).

Our composite fibers are composed of inexpensive, environmentally friendly, and biodegradable materials. The fibers themselves are sustainable because cellulose is highly abundant and coconut trees grow in many parts of the world. These trees can be replanted and therefore are a sustainable option. The fibers are a sustainable energy conversion source as an alternative to electrical appliances such as air conditioning, etc. While phase changing materials are reported in literature that involves expensive materials and synthetic routes (Chen et al. 2007; Fang et al. 2010; Fang and Zhang 2006; Fang et al. 2008; Meng

et al. 2015; Nelson 2002; Zhang et al. 2007), our smart composite fibrous material represents a sustainable alternative with a potential of being used in a broad range of applications such as smart textiles and other thermal insulation products.

Experimental section

Materials

Bleached high-pure sulfite spruce (softwood) cellulose pulp (SFI) with 95% α-cellulose content and 2% alkali-soluble content (degree of cellulose polymerization approx. 1100) was obtained from Weyerhaeuser Co. (2449 Stagecoach Rd, Oglethorpe, GA 31068 U.S.A). The RTIL 1-ethyl-3-methylimidazolium acetate ([EMIM][Ac]), absolute ethanol (≥ 99.8%) and analytical grade coconut oil were obtained from Sigma-Aldrich (St. Louis, Missouri, U.S.A). Double-distilled water (ddH$_2$O) was used for all the electrospinning experiments and subsequent washing steps.

Preparation of the fibers

Preparation of polymer solutions for electrospinning

Cellulose pulp was dissolved in [EMIM][Ac] by mechanical stirring at 80 °C to prepare a 1.5% (w/v) homogenous cellulose solution. Solidified coconut oil was melted by heating at 100 °C for 5 min.

Electrospinning procedure

The wet–wet electrospinning technique was used to construct the microfibers. All the electrospinning experiments were conducted inside an anti-static polycarbonate box designed and constructed in our lab. The CAD (Computer-aided design and drafting) model of the electrospinning box is shown in Fig. 1a. The entire electrospinning process was carried out in this box within a standard laboratory fume hood. All the experiments were carried out at 20±3 °C with a relative humidity of 48±5%. The temperature and the relative humidity were measured using a digital humidity and temperature monitor (AcuRite®). After a comprehensive literature review, the initial electrospinning parameters were selected from the following

ranges: concentration of cellulose from 1.5 to 2 w/v% (Hou et al. 2016; Miao et al. 2011; Miyauchi et al. 2010, 2011; Quan et al. 2010; Zheng et al. 2014); voltages from 15 to 20 kV (Hou et al. 2016; Liu and Hsieh 2002; Miao et al. 2011; Zheng et al. 2014, 2016); cellulose flow rate of 40 µL/min (Hou et al. 2016; Zheng et al. 2016); and distance of 9 cm (Miao et al. 2011; Miyauchi et al. 2010, 2011; Zheng et al. 2014, 2016). There is no reference for the flow rate of coconut oil since it has never been previously electrospun. There is an element of trial and error to finding optimal parameters for any specific electrospinning study (Quan et al. 2010; Vatankhah et al. 2014). The initial parameters were then optimized for this particular study to be: 1.5 w/v% concentration of cellulose; 18 kV voltage; 80 µL/min flow rate of cellulose; 10 µL/min flow rate of coconut oil; and 12.7 cm distance between the tip of the needle and the surface of the coagulation bath.

The coconut oil-cellulose core–shell microfibers were fabricated using the coaxial electrospinning technique. The schematic of the co-axial electrospinning apparatus is shown in Fig. 1b. A co-axial spinneret (MECC, Ogori, Fukuoka, Japan) was fitted with a blunt tip aluminum needle (23 Gauge) that has an internal diameter of 0.635 mm. The diameter of the outer needle was 2.50 mm. The 1.5% (w/v) cellulose solution (shell solution) and melted coconut oil (core solution) were placed in two separate 10 mL Norm-Ject syringes and connected to the spinneret using polytetrafluoroethylene (PTFE) tubing. A syringe heater kit (HEATER-KIT-1, New Era Pump System Inc., Wantagh, New York, U.S.A) was used to keep the melted coconut oil at a constant temperature of 80 °C. A high-voltage of 18 kV was applied between the spinneret (positive) and the electrically grounded collector (negative) using a high voltage supply (CZE1000R, Spellman, Hauppauge, New York, U.S.A) that is capable of generating a DC voltage up to 30 kV. The collector was a coagulation bath filled with 50% ethanol–water mixture with a small sheet of aluminum foil on the bottom. Pure ethanol and other highly flammable solvent baths must be avoided due to the risk of fire, as the frequent arcing is a source of ignition. Electrospun fibers were collected after the removal of the [EMIM][Ac] in the coagulation bath, which coagulated and solidified the fibers. The distance between the needle tip and the surface of the solution
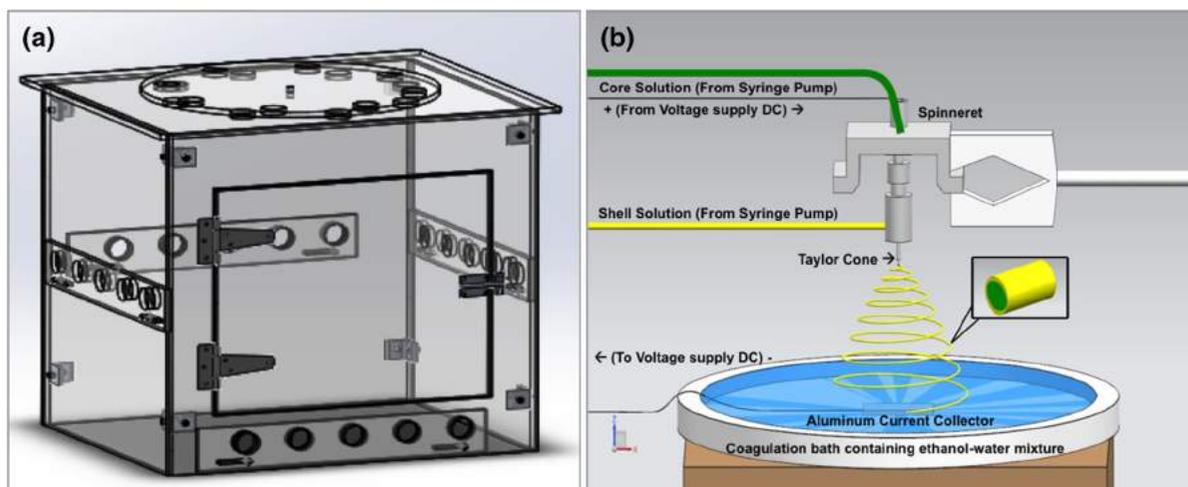
Fig. 1 Electrospinning set up. **a** Antistatic polycarbonate box, **b** Co-axial electrospinning set up

in the coagulation bath (spinning distance) was fixed at 12.7 cm. Two syringe pumps (NE-1000, New Era Pump System Inc., Wantagh, New York, U.S.A) were used to feed the core and shell polymer solutions at constant rates of 10 µL/min and 80 µL/min, respectively, to obtain continuous core–shell composite fibers. Finally, the fibers were washed several times with distilled and deionized water, and freeze-dried to obtain the final coconut oil-cellulose core–shell composite fiber balls.

Mono-axial electrospinning was used to fabricate cellulose microfibers as the negative control. The 1.5% (w/v) cellulose solution was placed in a 10 mL Norm-Ject syringe and connected to the mono-axial spinneret (MECC, Ogori, Fukuoka, Japan) using PTFE tubing. The spinneret was fitted with a blunt tip aluminum needle (23 Gauge) with an internal diameter of 0.635 mm. A high-voltage of 18 kV was applied while keeping the spinning distance fixed at 12.7 cm. The cellulose solution was pumped at a constant rate of 40 µL/min to obtain continuous monofilament fibers. Finally, the fibers were washed several times with water and freeze-dried to obtain the final cellulose microfiber balls.

Characterization

The amount of coconut oil inside the composite fibers was determined by crushing a known weight of fibers in hexane. This process forced the coconut oil to come out and get dissolved in hexane. Hexane was

later evaporated and the mass of coconut oil was obtained. The mass of composite fibers before the extraction and after corroborated the results. Carl Zeiss supra field emission scanning electron microscope (FESEM, Hillsboro, USA) was used to image the electrospun fiber samples at 1.5 kV (Resolution at 1 kV–2.5 nm). The average fiber diameters were determined from SEM images of over 200 individual fibers across 10 identical electrospinning experiments (Supporting Figure S1 & S2), using NIH Image J software (National Institute of Health, MD, USA). The core–shell fiber samples were further characterized using transmission electron microscopy (TEM). The samples were dispersed in ethanol, deposited on lacey carbon coated 200 mesh copper grids, and imaged at an accelerating voltage of 200 kV using the JEOL-JEM-2011 TEM (JEOL Ltd., Tokyo, Japan). The images were analyzed using NIH Image J software (National Institute of Health, MD, USA). Histograms representing the fiber size distribution were prepared using the Microsoft Excel™ software. Cellulose microfibers, coconut oil and coconut oil-cellulose core–shell composite fiber samples were subjected to thermogravimetric analysis (TGA) and differential scanning calorimetry (DSC). A computer-controlled TA Instruments TGA-Q50 apparatus (New Castle, Delaware, USA) was used to heat samples from room temperature to 800 °C at a constant heating rate of 5 °C/min under dry atmospheric conditions. Pre-weighed samples were sealed in hermetic aluminum pans and subjected to three
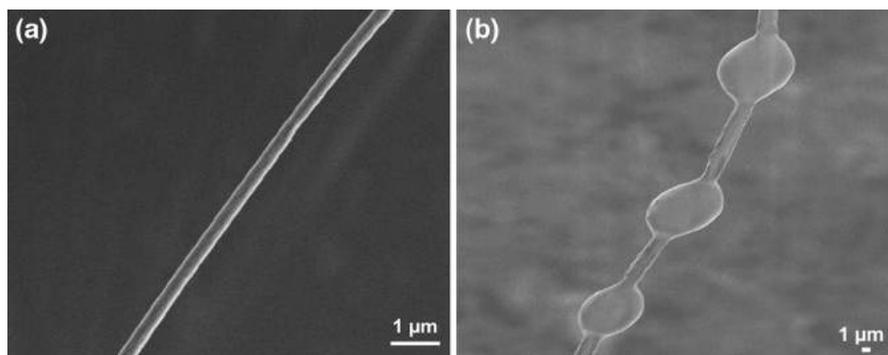
Fig. 2 Morphology of the electrospun microfibers. **a** SEM image of electrospun cellulose, Magnification-40,000, **b** SEM image of electrospun coconut oil-cellulose core–shell fibers, Magnification-4000

heating and cooling cycles between 0 and 45 °C at a constant heating rate of 1 °C/min. TA Instruments DSC-Q100 apparatus (New Castle, Delaware, USA) was used for this analysis.

Results and discussion

The wet–wet electrospinning technique was used to make cellulose and cellulose-coconut oil microfibers. An anti-static polycarbonate box was designed and constructed to isolate the electrospinning process from interference from static charges and the draft of the fume hood (Fig. 1a). Small ventilation windows were incorporated to accommodate solvent evaporation thereby keeping the humidity inside the box at $48 \pm 5\%$ throughout the electrospinning process. The co-axial electrospinning process used to fabricate coconut oil-cellulose core–shell microcomposite fibers is shown in Fig. 1b.

Initially, the cellulose-[EMIM][Ac] fiber jet forms an intermediate hydrogel upon entering the coagulation bath. This hydrogel state was formed due to the migration of RTIL into the water bath in exchange for water molecules (Hou et al. 2016). This process enables efficient removal of ionic liquid from the fiber. All the fibers collected in the coagulation bath were washed several times with distilled water and water/ethanol mixture under suction filtration to remove residual ionic liquid and other possible contaminants (Mahadeva and Kim 2012). During the washing steps fibers swell as expected to ensure effective removal of ionic liquid. Finally, the fibers were freeze-dried to obtain dry nonwoven microfiber

mats. Freeze-drying was preferred over air-drying to obtain a structure similar to cotton balls (Si et al. 2014; Zheng et al. 2016). The amount of coconut oil inside the composite fibers was determined to be around $76 \pm 10\%$ based on the total mass of the composite fibers.

The cellulose monofilament fibers (negative control) appeared to have a continuous cylindrical structure (Fig. 2a and SD, Fig. 1) with an average diameter of 600 ± 200 nm (Fig. 3a), which is consistent with prior art (Kim et al. 2006). However, the coconut oil–cellulose composite fiber morphology was quite dissimilar from typical cellulose fibers. The composite fibers appeared to have a beaded structure with alternating cylindrical and biconical shaped regions (Fig. 2b and SD, Fig. 2). The average diameter of the fibers excluding the biconical regions was 3000 ± 1000 nm (Fig. 3b). The fabrication process for the composite was developed through a trial and error approach using a range of different electrospinning parameters. In each instance that core–shell behavior was observed, the composite exhibited a beaded structure. All other instances resulted in hollow fibers without coconut oil confined inside the fibers or neat cellulose fibers. The beaded nature of the composite is likely due to the differences in material properties between cellulose and coconut oil. Cellulose, having many polar functional groups, has a much higher surface energy (67 mJ m^2) (Miller and Donald 2002) than the hydrophobic coconut oil (24 mJ m^2) (Thangaraja et al. 2016). In order for the free energy of the composite to be minimized, the contact area between the cellulose and coconut oil needs to be minimized
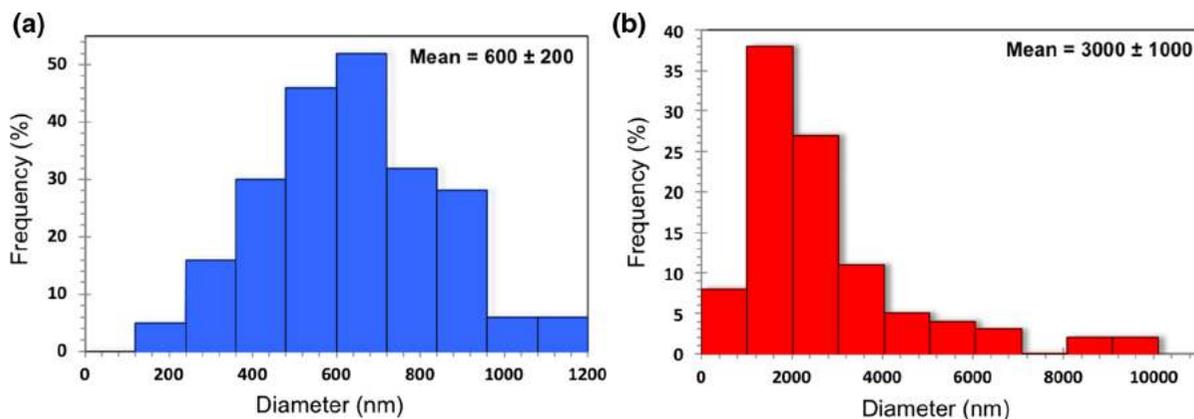
Fig. 3 Histograms of the diameters of cellulose microfibers (a) and coconut oil-cellulose core–shell microfibers excluding the biconical regions (b) observed during SEM imaging

due to the mismatch of surface energies. This likely caused the coconut oil to aggregate into nearly spherical beads as a sphere has the lowest surface area to volume ratio. This is the reason the authors theorize that after many trial and error attempts only beaded core–shell fibers were observed. Therefore, the window in which the electrospinning parameters could be tuned was very narrow. Nevertheless, this procedure resulted in consistent coconut oil-cellulose core–shell beaded composite fibers and was observed throughout all the fibers. Coconut oil is also present throughout the core of the fibers but is mostly concentrated in the biconical structures.

The SEM image in Fig. 4a displays the physical appearance of the surface of a biconical region, which closely resembles the wrinkled appearance of the surface of typical electrospun cellulose microfibers (Zheng et al. 2014, 2016). The core–shell structure of the coconut oil–cellulose composite fiber is revealed in the TEM image shown in Fig. 4b. Hydrophobic coconut oil seems to be concentrated in the center of

the fiber and occupy most of the space inside. Both cellulose and coconut oil have similar elemental compositions, making the electron beam interact similarly with each component in bright field imaging. Therefore, the bright contrast comes from the differences in density and thickness of the sample. In thicker samples, fewer electrons reach the detector. There are three distinct regions visible in the TEM images of the composite fibers. The thinner outermost shell (~400 nm) appears to be densely packed cellulose and the less dense coconut oil makes the innermost core (~3.70 μm) to be brighter in contrast to the shell. In between lies a region with both cellulose and coconut oil.

In conventional wet-dry coaxial electrospinning, polymers are dissolved in volatile organic solvents, which rapidly evaporate upon the exit of the fiber jet from the needle. The quick evaporation of the volatile organic solvents allows for less mixing of the two components and "freezes" the core–shell structure almost instantaneously. This provides a sharp
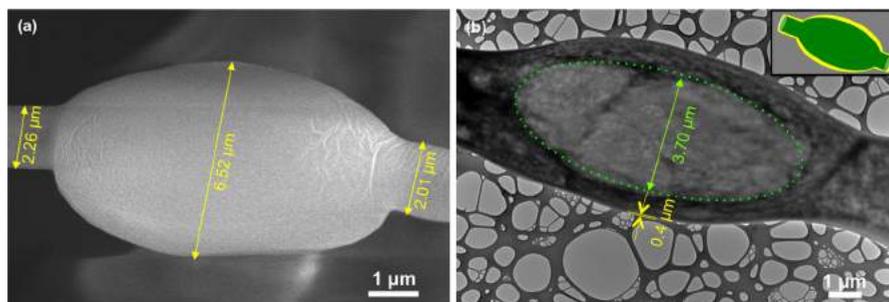

Fig. 4 Biconical and co-axial structure of coconut oil–cellulose core–shell fibers. a SEM, b TEM images

contrast between the core and shell regions in the TEM images. The current study employs wet–wet electrospinning, where a non-volatile RTIL solvent is used. Fiber formation occurs through precipitation in the coagulation bath through an intermediate hydrogel state, not by solvent evaporation. This process allows for greater time for diffusion between the core and shell materials, creating an intermediate region where both substances are present in significant quantities. This intermediate hydrogel that forms in the coagulation bath allows time for changes in the structural morphology of the composite fibers. The authors have not come across examples of this intermediate region between the core and the shell due to the infrequent use of wet–wet coaxial electrospinning. The formation of the beads could be due the clustering of oil inside the fiber due to hydrophobic interactions that repel the highly polar cellulose shell in order to minimize contact area.

The diameters of the biconical region were measured across the center of the structure with the largest perimeter. These biconical structures have an average diameter of 8000±4000 nm (Fig. 5). Assuming a normal distribution of bead sizes with mean diameter of 8 μm and standard deviation of 4 μm (cf. Figure 5), the bead diameter will be less than 16 μm with 95% confidence. The standard deviation of the fiber diameter in wet–wet electrospinning is typically much broader than wet-dry electrospinning as previously reported (Greiner and Wendorff 2007; Hou et al. 2016; Lee et al. 2002; Li et al. 2006).

Coconut oil, cellulose and composite fibers were subjected to thermogravimetric analysis where they were heated from 20–800 °C at a constant heating rate of 5 °C per minute under dry atmospheric conditions. The thermograms in Fig. 6a and b show that the coconut oil possesses better thermal stability than either cellulose or composite fibers, and only starts to decompose (onset temperature) at~233 °C. In contrast, the coconut oil-cellulose core–shell fibers start to decompose at the lowest temperature (i.e.~150 °C) with a maximum decomposition rate of 4% per minute at 294 °C. Cellulose microfibers start to decompose at~190 °C and show the highest rate of degradation (i.e. 13%/minute at 294 °C). Although the onset of decomposition was at a lower temperature for the composite compared with neat cellulose, the composite showed significantly slower decomposition rate. This is more evident from the residual
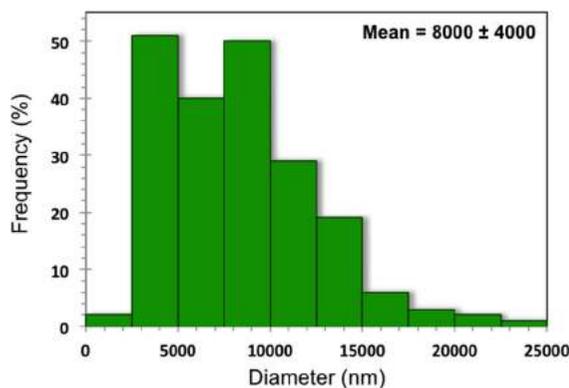

Fig. 5 Histograms of the diameters of only the biconical regions of the core–shell fibers observed during SEM and TEM imaging

mass left behind by each sample at the end of the heating process. Cellulose microfibers left the highest amount of residue (i.e. 12%) at 800 °C. Core–shell fibers showed a residual mass of 3% and coconut oil (Mosarof et al. 2016) left no residue behind. However, both cellulose and coconut oil-cellulose core–shell fibers appeared to be thermally stable below 190 °C, which includes the desired temperature range for the thermo-regulating microcomposite fiber product. The absence of decomposition peaks of potential contaminants such as hemicellulose (~220 °C) (Werner et al. 2014) and lignin (~100 °C) (Watkins et al. 2015) corroborate the manufacturer's reported purity of the cellulose fibers.

The derivative thermogravimetric (DTG) curves (Fig. 6b) show the average decomposition temperatures that correlate to different mass losses that occur during heating of these samples. Cellulose microfibers showed a small peak around 43 °C. This mass reduction is likely due to the loss of physically absorbed water in the fiber. Both cellulose and coconut oil cellulose core–shell fibers showed two major weight losses at 294 °C and ~450 °C that correspond to the combustion and smoldering of cellulose (Zheng et al. 2014). Coconut oil-cellulose core–shell fibers also showed another significant weight loss at 210 °C. Coconut oil showed two major weight losses at 323 and 497 °C.

The purpose of coconut oil in the core–shell fibers is to regulate the temperature of the immediate environment. When the surrounding temperature is warm (i.e. above the melting point of oil) the coconut
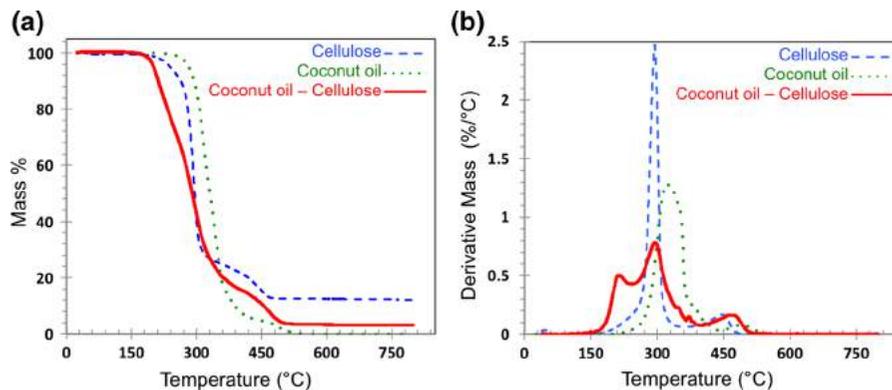
Fig. 6 TGA analysis. **a** Mass % versus temperature **b** derivative mass versus temperature

oil absorbs heat and melts, when the surrounding temperature is cold (i.e. below the melting point of oil) coconut oil releases heat by crystallizing inside the fiber. Cellulose acts as a solid hydrophilic shell to hold the hydrophobic oil core in place. Depending on the end use, the shell composition can be altered with other materials to make it more strong and flexible. DSC analysis was used to determine the phase transition properties of coconut oil and coconut oil–cellulose core–shell fibers. The DSC thermograms of coconut oil and coconut oil-cellulose core–shell microcomposite fibers are shown in Fig. 7. Three different exotherms and endotherms for each sample were obtained by subjecting the samples to three consecutive heating and cooling cycles between 0 and 45 °C. DSC thermograms of cellulose showed no peaks for both heating and cooling cycles. The complete DSC thermograms of electrospun cellulose, coconut oil and coconut oil-cellulose core–shell microfibers are shown in SD, Fig. 3.

Cellulose is a mechanically robust polysaccharide that does not melt below 400 °C (Krumm et al. 2016) but starts to thermally decompose at around 190 °C (Jiang et al. 2017). Both neat coconut oil and coconut oil encapsulated inside the core–shell fibers showed a broad melting peak with shoulders starting from 1.8 to 29 °C. This corresponds to the phase transition of solid coconut oil to liquid (Mosarof et al. 2016). Confined coconut oil and neat coconut oil showed average melting points (T_m) at around 22.0 ± 0.1 °C and 23.0 ± 0.1 °C, respectively (Mosarof et al. 2016) (Table 1). They also showed two distinct crystallization peaks that displayed significantly different maximum specific heat flows (Fig. 7). This behavior

is due to coconut oil being a multi component mixture of a few different mono and poly-unsaturated fatty acids with slightly different melting and crystallization points (Jayadas and Nair 2006). The first crystallization peak for neat coconut oil revealed an average temperature of (T_c1) 15.0 ± 0.1 °C. In contrast, the second crystallization peak has an average temperature of (T_c2) 9.0 ± 0.2 °C. When the coconut oil was inside the fiber, it showed T_c1 (14.0 ± 1.0 °C) and T_c2 (8.0 ± 0.1 °C) values similar to those of neat coconut oil. However, both melting and crystallization points showed a one-degree reduction for the coconut oil inside the axial pore. This decrease of melting and crystallization temperatures of coconut oil inside the fibers can be explained by the thermoporometry based on Gibbs–Thomson thermodynamic relationship (Chen et al. 2009). The equilibrium temperature for a solid–liquid transition is determined by the radius of curvature of the interface between the solid and liquid phases. When a liquid is held inside a pore, the radius of curvature is closely related to the pore size (Landry 2005). Thermoporometry depicts the relationship between the pore size and the depression of melting or crystallization point of the liquid in the pore. Crystallization of neat coconut oil took place over a narrow temperature range starting from 6.2 °C and ending at 16.5 °C. But coconut oil inside the core–shell fiber exhibited a broader crystallization range starting from 0.3 to 16.5 °C. This could be due to limited mobility of fatty acid chains in the core of the fiber that resulted in the formation of a wide distribution of crystallite sizes (Unruh et al. 1999).

Fig. 7 DSC endotherms (**a**, **b**) and exotherms (**c**, **d**) of coconut oil both outside (**a**, **c**) and inside (**b**, **d**) of the core–shell fibers
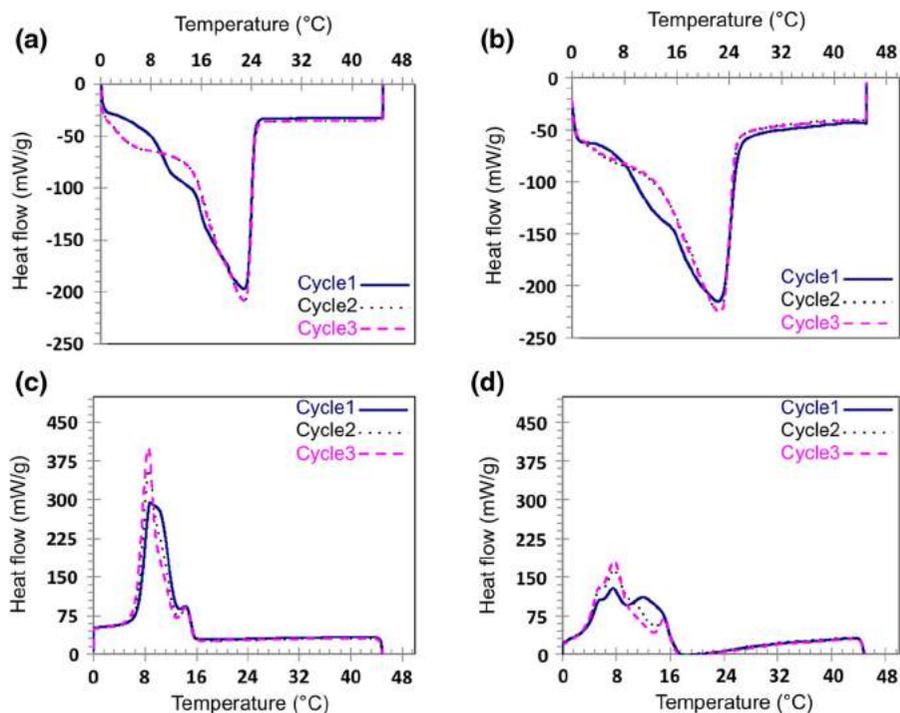

Table 1 Average temperature of melting (T_m) and crystallization (T_c), specific heat (ΔH) and specific heat capacity (C_p) along with the standard deviation values of solid oil and the liquid calculated from the DSC thermograms

	T_m (°C)	T_c1 (°C)	T_c2 (°C)	ΔH (J/g)		C_p (J/g. °C)	
				ΔH_m	ΔH_c	Solid	Liquid
Neat coconut oil	23.0±0.1	15.0±0.1	9.0±0.2	95.7±2.4	66.0±1.6	1.77±0.2	2.05±0.1
Coconut oil inside the microfibers	22.0±0.1	14.0±1.0	8.0±0.1	134.9±6.6	64.7±1.5	3.50±0.3	2.55±0.1
Change in thermal properties	−1.0	−1.0	−1.0	+39.2	−1.3	+1.73	+0.50

The specific heat (ΔH; J/g) of phase transitions was calculated using graphs of each sample plotting specific heat rate (J/s.g) as a function of time (s). Three different specific heat values were calculated using three different cooling and heating cycles and the average specific heat of melting (ΔH_m) and crystallization (ΔH_c) were determined. All the melting and crystallization peaks contain shoulders that allow splitting of the peak into segments. All the cooling and heating thermograms showed four different segments except for the neat coconut oil exotherms, which can only be split into three segments. ΔH values were calculated for each segment ($\Delta H1$, 2 and 3). The derivative specific heat flow (W/g. °C) graphs of each cycle were used to determine the temperature limits for each segment

(SD, Fig. 4, 5). The specific heat values calculated from each segment were added to obtain the ΔH_m and ΔH_c values for each cycle and later averaged to obtain final average ΔH_m and ΔH_c for both coconut oil and the coconut oil inside the core–shell fibers. Finally, the specific heat capacities (C_p) of the solid oil and liquid were calculated from the equation (Cao 1999) below. The equation shows the relationship between C_p, heating rate (r; °C/min), sample mass (m;mg) and the heat flow of the base line (a;mW).

$$C_p = 60a \div mr$$

The average ΔH_m, ΔH_c and C_p values for both neat coconut oil and the coconut oil inside the core–shell fibers are shown in Table 1. The DSC data for the

composite was normalized by the weight of the coconut oil present in the fibers and not by the total mass of the fibers. The mass of the coconut oil was chosen as the normalization parameter for the composite fibers because neat cellulose does not have a phase transitions in the range of 0 and 45 °C. This facilitates the comparison between the specific heats of unconfined and confined coconut oil.

The calculated ΔH_m value of coconut oil inside the core–shell fiber is 39.2 J/g greater than that of neat coconut oil (Mosarof et al. 2016) (Table 1). In both cases the specific heat of melting decreases with increasing number of heating cycles. However, the calculated ΔH_c value of coconut oil inside the core–shell fiber, 64.7 J/g, is slightly less than (1.3 J/g) that of neat coconut oil, 66.0 J/g. This reduction could be due to the change in the arrangement of the fatty acid molecules to a less energetically favorable structure. When the coconut oil is confined to the core of the fiber the polymeric chains have limited movement (Huang et al. 2013). Hence, coconut oil will not achieve its most stable solid-state form, consequently releasing less energy to the surroundings. An interesting trend was evident in the crystallization peak height of both peaks observed in the exotherms of coconut oil. The height of the taller peak increases with increasing number of cycles and the opposite can be seen with regard to the shorter peak (i.e. the height decreases with increasing number of cycles). This could be due to the fact that with each cooling cycle, the fatty acid molecules are achieving a more energetically favorable spatial arrangement that crystallizes closer to T_c2.

The specific heat capacities of the solid and liquid coconut oil are comparable to the reported data in the literature (Putri et al. 2016). However, the specific heat capacities of the oil inside the fiber showed an interesting increase compared to neat oil. The calculated C_p of solid and liquid oil inside the core–shell fiber was 1.73 J/g. °C and 0.50 J/g. °C greater than that of neat coconut oil. Over the course of three consecutive heating–cooling cycles between 0 and 45 °C, the composite was thermally stable as it showed specific heat capacity consistent with confined coconut oil. This is only possible if the composite remained intact and the coconut oil did not leach to the exterior of the fiber, in which case the coconut oil would have a specific heat capacity equivalent to neat coconut oil. As a rough estimate

based on the SEM and TEM images of the composite fiber dimensions, there are ~1 million composite fibers inside a DSC pan for the thermal experiment. In addition, the thermal experiments were run in triplicate, yielding thermal properties derived from millions of fibers. This means any fiber-to-fiber variations are averaged out and included in the overall material performance reported. It is impossible to have every fiber be exactly the same due to the inherent stochastic nature of electrospinning.

Conclusions

Temperature-regulating fibrous material was developed using co-axial electrospinning of biomass. This fibrous composite material was then used as a model system to study the thermal behavior of the naturally occurring PCM coconut oil inside a solid cellulose fiber. Coconut oil in the core of the fibers showed excellent phase changing properties in the temperature range from 7 to 22 °C. When coconut oil was confined to a smaller axial micropore, the specific heat capacity of solid and liquid oil was increased by 98 and 24%, respectively, compared with when the oil was unconfined. It also showed a significant increase of 41% in specific heat of melting with a minor 2% decrease in the specific heat of crystallization. Furthermore, this material has the capability to store relatively large amounts of heat over a narrow temperature range without a noticeable volume change while maintaining the temperature of the immediate environment below 22 °C and above 7 °C. Different oil or mixtures of oils may be used to customize the temperature range depending on the end user requirements. The authors hypothesize these core–shell fibers can also be developed into more resilient material by modifying the shell of the fibers with harder and more elastic materials. Use of different polymers in the shell would likely change the properties and the applications of the composite material. Certain applications may require crosslinking of the shell polymer to add extra strength to the fibers (Chen et al. 2009). There are also other applications in which these composite fibers would be envisioned to be included as a component inside a supporting matrix providing mechanical support in thermoregulating systems. This would potentially

enable a broader range of applications in the textile industry for novel thermal insulation materials.

Author's Contributions The study was performed by W.M.R. N.U., C.F.W., C.M. and C.C. and the manuscript was written by W.M.R.N.U. & R.J.L. All authors have given their approval to the final version of this manuscript.

Compliance with ethical standards

Conflict of interest All authors declares that they do not have conflict of interest.

References

Abhat A (1983) Low temperature latent heat thermal energy storage: heat storage materials. Sol Energy 30:313–332

Ajithkumar G, Jayadas N, Bhasi M (2009) Analysis of the pour point of coconut oil as a lubricant base stock using differential scanning calorimetry. Lubr Sci 21:13–26

Arioli T, Peng L, Betzner AS, Burn J, Wittke W, Herth W, Camilleri C, Höfte H, Plazinski J, Birch R (1998) Molecular analysis of cellulose biosynthesis in arabidopsis. Science 279:717–720

Boardman B (2013) Fixing fuel poverty: challenges and solutions. Routledge, London

Cadarette BS, Cheuvront SN, Kolka MA, Stephenson LA, Montain SJ, Sawka MN (2006) Intermittent microclimate cooling during exercise-heat stress in us army chemical protective clothing. Ergonomics 49:209–219

Cao J (1999) Mathematical studies of modulated differential scanning calorimetry: I. Heat capacity measurements. Thermochim Acta 325:101–109

Chen C, Wang L, Huang Y (2007) Electrospinning of thermo-regulating ultrafine fibers based on polyethylene glycol/cellulose acetate composite. Polymer 48:5202–5207

Chen C, Wang L, Huang Y (2009) Crosslinking of the electrospun polyethylene glycol/cellulose acetate composite fibers as shape-stabilized phase change materials. Mater Lett 63:569–571

Chen Z, Wang P, Wei B, Mo X, Cui F (2010) Electrospun collagen–chitosan nanofiber: A biomimetic extracellular matrix for endothelial cell and smooth muscle cell. Acta Biomater 6:372–382

Chen C, Wang L, Huang Y (2011) Electrospun phase change fibers based on polyethylene glycol/cellulose acetate blends. Appl Energy 88:3133–3139

Cooley JF (1902) Apparatus for electrically dispersing fluids. U.S. Patent US692631A, 1902

Coyle S, Wu Y, Lau K-T, De Rossi D, Wallace G, Diamond D (2007) Smart nanotextiles: a review of materials and applications. MRS Bull 32:434–442

Fang X, Zhang Z (2006) A novel montmorillonite-based composite phase change material and its applications in thermal storage building materials. Energy Build 38:377–380

Fang Y, Kuang S, Gao X, Zhang Z (2008) Preparation and characterization of novel nanoencapsulated phase change materials. Energy Convers Manage 49:3704–3707

Fang G, Chen Z, Li H (2010) Synthesis and properties of microencapsulated paraffin composites with sio 2 shell as thermal energy storage materials. Chem Eng J 163:154–159

Farid MM, Khudhair AM, Razack SAK, Al-Hallaj S (2004) A review on phase change energy storage: materials and applications. Energy Convers Manage 45:1597–1615

Farrán A, Cai C, Sandoval M, Xu Y, Liu J, Hernáiz MJ, Linhardt RJ (2015) Green solvents in carbohydrate chemistry: from raw materials to fine chemicals. Chem Rev 115:6811–6853

Flouris AD, Cheung SS (2006) Design and control optimization of microclimate liquid cooling systems underneath protective clothing. Ann Biomed Eng 34:359

Freire MG, Teles ARR, Ferreira RA, Carlos LD, Lopes-da-Silva JA, Coutinho JA (2011) Electrospun nanosized cellulose fibers using ionic liquids at room temperature. Green Chem 13:3173–3180

Frenot A, Henriksson MW, Walkenström P (2007) Electrospinning of cellulose-based nanofibers. J Appl Polym Sci 103:1473–1482

Greiner A, Wendorff JH (2007) Electrospinning: A fascinating method for the preparation of ultrathin fibers. Angew Chem Int Edit 46:5670–5703

Hasnain S (1998) Review on sustainable thermal energy storage technologies, part I: heat storage materials and techniques. Energy Convers Manage 39:1127–1138

Hou L, Udangawa WRN, Pochiraju A, Dong W, Zheng Y, Linhardt RJ, Simmons TJ (2016) Synthesis of heparin-immobilized, magnetically addressable cellulose nanofibers for biomedical applications. ACS Biomater Sci Eng 2:1905–1913

Huang H-D, Xu J-Z, Fan Y, Xu L, Li Z-M (2013) Poly (l-lactic acid) crystallization in a confined space containing graphene oxide nanosheets. J Phys Chem B 117:10641–10651

Huang F, Xu Y, Peng B, Su Y, Jiang F, Hsieh Y-L, Wei Q (2015) Coaxial electrospun cellulose-core fluoropolymer-shell fibrous membrane from recycled cigarette filter as separator for high performance lithium-ion battery. ACS Sustain Chem Eng 3:932–940

Iqbal K, Sun D (2014) Development of thermo-regulating polypropylene fibre containing microencapsulated phase change materials. Renew Energy 71:473–479

Jaganathan SK, Fauzi Ismail A (2017) Production and hemocompatibility assessment of novel electrospun

polyurethane nanofibers loaded with dietary virgin coconut oil for vascular graft applications. J Bioact Compat Polym 33:210–223

Jayadas N, Nair KP (2006) Coconut oil as base oil for industrial lubricants—evaluation and modification of thermal, oxidative and low temperature properties. Tribol Int 39:873–878

Jiang Z, Chen D, Yu Y, Miao J, Liu Y, Zhang L (2017) Composite fibers prepared from multi-walled carbon nanotubes/cellulose dispersed/dissolved in ammonium/dimethyl sulfoxide mixed solvent. RSC Adv 7:2186–2192

Khalil HA, Bhat A, Yusra AI (2012) Green composites from sustainable cellulose nanofibrils: a review. Carbohyd Polym 87:963–979

Kim C-W, Kim D-S, Kang S-Y, Marquez M, Joo YL (2006) Structural studies of electrospun cellulose nanofibers. Polymer 47:5097–5107

Krumm C, Pfaendtner J, Dauenhauer PJ (2016) Millisecond pulsed films unify the mechanisms of cellulose fragmentation. Chem Mater 28:3108–3114

Lalia BS, Guillen-Burrieza E, Arafat HA, Hashaikeh R (2013) Fabrication and characterization of polyvinylidenefluoride-co-hexafluoropropylene (pvdf-hfp) electrospun membranes for direct contact membrane distillation. J Membrane Sci 428:104–115

Lan T, Shao Z-Q, Wang J-Q, Gu M-J (2015) Fabrication of hydroxyapatite nanoparticles decorated cellulose triacetate nanofibers for protein adsorption by coaxial electrospinning. Chem Eng J 260:818–825

Landry MR (2005) Thermoporometry by differential scanning calorimetry: experimental considerations and applications. Thermochim Acta 433:27–50

Lee KH, Kim HY, La YM, Lee DR, Sung NH (2002) Influence of a mixing solvent with tetrahydrofuran and n, n-dimethylformamide on electrospun poly (vinyl chloride) nonwoven mats. J Polym Sci Pol Phys 40:2259–2268

Li Y, Huang Z, Lǚ Y (2006) Electrospinning of nylon-6, 66, 1010 terpolymer. Eur Polym J 42:1696–1704

Li F, Zhao Y, Song Y (2010) Core-shell nanofibers: nano channel and capsule by coaxial electrospinning. In: Kumar A (ed) nanofibers. InTech, Croatia, pp 419–438

Liebert T (2010) Cellulose solvents-remarkable history, bright future. In: Liebert TF, Heinze TJ, Edgar KJ (eds) Cellulose solvents: for analysis, shaping and chemical modification, vol 1033. Acs symposium series. Oxford University Press, Oxford, pp 3–54

Liu H, Hsieh YL (2002) Ultrafine fibrous cellulose membranes from electrospinning of cellulose acetate. J Polym Sci Pol Phys 40:2119–2129

Mahadeva SK, Kim J (2012) Influence of residual ionic liquid on the thermal stability and electromechanical behavior of cellulose regenerated from 1-ethyl-3-methylimidazolium acetate. Fiber Polym 13:289–294

McCann JT, Marquez M, Xia Y (2006) Melt coaxial electrospinning: a versatile method for the encapsulation of solid materials and fabrication of phase change nanofibers. Nano Lett 6:2868–2872

Meli L, Miao J, Dordick JS, Linhardt RJ (2010) Electrospinning from room temperature ionic liquids for biopolymer fiber formation. Green Chem 12:1883–1892

Meng Q, Li G, Hu J (2015) Phase change fibers and assemblies. In: Tao X (ed) Handbook of smart textiles. Springer, Singapore, pp 225–251

Miao J, Pangule RC, Paskaleva EE, Hwang EE, Kane RS, Linhardt RJ, Dordick JS (2011) Lysostaphin-functionalized cellulose fibers with antistaphylococcal activity for wound healing applications. Biomaterials 32:9557–9567

Miller AF, Donald AM (2002) Surface and interfacial tension of cellulose suspensions. Langmuir 18:10155–10162

Miyauchi M, Miao J, Simmons TJ, Lee J-W, Doherty TV, Dordick JS, Linhardt RJ (2010) Conductive cable fibers with insulating surface prepared by coaxial electrospinning of multiwalled nanotubes and cellulose. Biomacromol 11:2440–2445

Miyauchi M, Miao J, Simmons T, Dordick J, Linhardt R (2011) Flexible electrospun cellulose fibers as an affinity packing material for the separation of bovine serum albumin. J Chromatogr Sep Tech 2:110

Mondal S (2008) Phase change materials for smart textiles–an overview. Appl Therm Eng 28:1536–1550

Mosarof M, Kalam M, Masjuki H, Arslan A, Monirul I, Ruhul A, Shahir S, Khuong L (2016) Analysis of thermal stability and lubrication characteristics of millettia pinnata oil. RSC Adv 6:81414–81425

Nejman A, Goetzendorf-Grabowska B (2013) Heat balance of textile materials modified with the mixtures of pcm microcapsules. Thermochim Acta 569:144–150

Nelson G (2002) Application of microencapsulation in textiles. Int J Pharm 242:55–62

Putri WA, Fahmi Z, Sutjahja I, Kurnia D, Wonorahardjo S (2016) Thermophysical parameters of coconut oil and its potential application as the thermal energy storage system in indonesia. J Phys: Conf Ser 739:012065

Quan S-L, Kang S-G, Chin I-J (2010) Characterization of cellulose fibers electrospun using ionic liquid. Cellulose 17:223–230

Si Y, Yu J, Tang X, Ge J, Ding B (2014) Ultralight nanofibre-assembled cellular aerogels with superelasticity and multifunctionality. Nat Commun 5:5802

Simmons TJ, Lee SH, Miao J, Miyauchi M, Park T-J, Bale SS, Pangule R, Bult J, Martin JG, Dordick JS (2011) Preparation of synthetic wood composites using ionic liquids. Wood Sci Technol 45:719–733

Swatloski RP, Spear SK, Holbrey JD, Rogers RD (2002) Dissolution of cellose with ionic liquids. J Am Chem Soc 124:4974–4975

Teo WE, Ramakrishna S (2006) A review on electrospinning design and nanofibre assemblies. Nanotechnology 17:R89

Thangaraja J, Anand K, Mehta PS (2016) Predicting surface tension for vegetable oil and biodiesel fuels. RSC Adv 6:84645–84657

Unruh T, Bunjes H, Westesen K, Koch MH (1999) Observation of size-dependent melting in lipid nanoparticles. J Phys Chem B 103:10373–10377

Vatankhah E, Semnani D, Prabhakaran MP, Tadayon M, Razavi S, Ramakrishna S (2014) Artificial neural network for modeling the elastic modulus of electrospun polycaprolactone/gelatin scaffolds. Acta Biomater 10:709–721

Vigo TL, Frost C (1982) Temperature-sensitive hollow fibers containing phase change salts. Text Res J 52:633–637

Vigo TL, Frost CM (1983) Temperature adaptable hollow fibers containing polyethylene glycols. J Coat Fabr 12:243–254

Viswanathan G, Murugesan S, Pushparaj V, Nalamasu O, Ajayan PM, Linhardt RJ (2006) Preparation of biopolymer fibers by electrospinning from room temperature ionic liquids. Biomacromol 7:415–418

Walker JW (2009) Ask the experts: When air is the same temperature as our body, why do we feel hot? Sci Am 300:84

Watkins D, Nuruddin M, Hosur M, Tcherbi-Narteh A, Jeelani S (2015) Extraction and characterization of lignin from different biomass resources. J Mater Res Technol 4:26–32

Werner K, Pommer L, Broström M (2014) Thermal decomposition of hemicelluloses. J Anal Appl Pyrol 110:130–137

Yu D, Wang X, Li X, Chian W, Li Y, Liao Y (2013a) Electrospun biphasic drug release polyvinylpyrrolidone/ethyl cellulose core/sheath nanofibers. Acta Biomater 9:5665–5672

Yu D-G, Chian W, Wang X, Li X-Y, Li Y, Liao Y-Z (2013b) Linear drug release membrane prepared by a modified coaxial electrospinning process. J Membrane Sci 428:150–156

Zhang Y, Zhou G, Lin K, Zhang Q, Di H (2007) Application of latent heat thermal energy storage in buildings: state-of-the-art and outlook. Build Environ 42:2197–2209

Zheng Y, Miao J, Maeda N, Frey D, Linhardt RJ, Simmons TJ (2014) Uniform nanoparticle coating of cellulose fibers during wet electrospinning. J Mater Chem A 2:15029–15034

Zheng Y, Cai C, Zhang F, Monty J, Linhardt RJ, Simmons TJ (2016) Can natural fibers be a silver bullet? Antibacterial cellulose fibers through the covalent bonding of silver nanoparticles to electrospun fibers. Nanotechnology 27:055102